JTTEE5 14:231-238
DOI: 10.1361/105996304523809
1059-9630/$19.00 © ASM International

Young's Modulus and Fatigue Behavior of Plasma-Sprayed Alumina Coatings

O. Kovářík, J. Siegl, J. Nohava, and P. Chráska

(Submitted July 17, 2003; in revised form October 3, 2003)

The fatigue behavior and Young's modulus of plasma-sprayed gray alumina on low-carbon steel substrates were investigated. The investigation of the properties of composites that were defined as "coating-substrate" composites included measurements of the microhardness profile, the residual stress on the top of the coating, and the residual stress profile in the substrate. Fatigue samples were periodically loaded as a cantilever beam on a special testing machine. Failed samples were observed with a scanning electron microscope to determine the failure processes in the coating. The Young's modulus of the coating was measured by the four-point bending method. Samples were tested both in tension and compression under low (300 N) and high (800 N) loads. The authors' experiments revealed that the average fatigue lives of coated specimens were nearly two times longer than those of the uncoated specimens. The measurements of Young's modulus of the coating yielded values that varied between 27 and 53 GPa, with an average value of 43 GPa. Loading in tension caused a decrease in the Young's modulus of the coating, while loading in compression led to an increase in Young's modulus. The increase in the lifetime of coated samples was likely due to compressive residual stresses in the substrate, originating during the spray process. The failure of the coating was due to several processes, among which the most important were splat cracking, splat debonding, and the coalescence of cracks through the voids in the coating.

Keywords alumina, fatigue, plasma spray, Young's modulus

1. Introduction

Thermal spray coatings can be the solution to improving the mechanical properties of construction materials while saving weight. At the same time, the fatigue properties of coated bodies are gaining importance due to an increasing number of aeronautical, medical, and other applications. An experimental program aimed to find properties that have an essential influence on fatigue resistance and to find methods for measuring such properties. Several experimental methods, including microhardness measurement, x-ray residual stress measurement, in situ bending in a scanning electron microscope (SEM) vacuum chamber, fractography, and metallography, were used for the characterization of "substrate-coating" composites.

The Young's modulus of plasma-sprayed coatings as well as the fatigue properties of a material are characteristics that are indispensable for the designers of construction parts. Furthermore, there is increasing evidence in the literature concerning the variation in Young's modulus of the coatings when they are subjected to higher loads (Ref 1, 2). In the present experiments, the focus was not only on the measurements of Young's modulus of plasma-sprayed alumina coatings, but also on the behavior of Young's modulus at increasing deformations of up to 0.3%.

O. Kovářík and **J. Siegl,** Department of Materials, Faculty of Nuclear Sciences and Physical Engineering, Czech Technical University, Prague, Czech Republic; and **J. Nohava** and **P. Chráska,** Institute of Plasma Physics, Academy of Sciences of the Czech Republic, Prague, Czech Republic. Contact e-mail: kovarik@kmat.fjfi.cvut.cz.

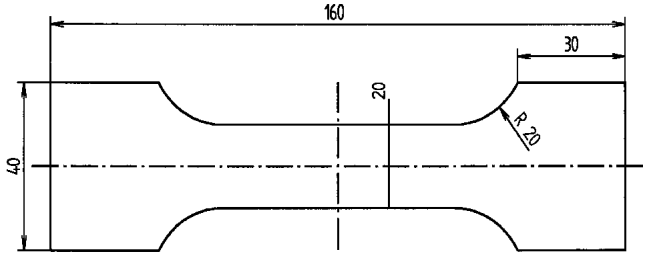

Fig. 1 The geometry of the specimen used in the fatigue test (all dimensions are in millimeters). The specimen is viewed from the spray direction.

2. Experimental Methods

All substrates were made from low-carbon steel with a thickness of 4 or 2.5 mm. The substrates for fatigue testing were machined to the dimensions shown in Fig. 1. Young's modulus measurements required rectangular samples with dimensions of 120 by 20 mm. Five different sets of fatigue specimens and two sets of Young's modulus specimens were prepared (Table 1).

Al_2O_3 powder with particles of a mean size of 600 μm was used for grit blasting. Other methods for substrate cleaning were not used. Alumina coatings were sprayed using the WSP 160 water-stabilized plasma system (ÚFP Praha, Czech Republic) immediately after grit blasting. The torch was powered with about 160 kW (320 V, 500 A). The feedstock material was crushed alumina powder (AH 230 and AH 240, Carborundum Electrite, Benátky n. Jizerou, Czech Republic), which is specified in Table 1. The distance of the plasma torch from the specimen was 350 mm, and the preheat temperature of the substrate, measured by optical pyrometer, was 120 °C. The feeding rate was 26 kg/h, and the linear transversal speed was 29 cm/s. The

Table 1 The different series of specimens

Set	Powder	Coating thickness, mm	Substrate thickness, mm	Grit-blasted	Loading	Comments
P	…	…	4	No	Fatigue	Plain sample
TA	…	…	4	Yes	Fatigue	Grit-blasted sample
1A	AH240(a)	0.35	4	Yes	Fatigue	PS sample, both sides coated
2A	AH230(b)	0.8	4	Yes	Fatigue	PS sample, both sides coated
3A	AH240(a)	0.9	4	Yes	Fatigue	PS sample, both sides coated
1A25	AH240(a)	0.35	2.5	Yes	4PB	PS sample, one side coated
1A40	AH240(a)	0.35	4	Yes	4PB	PS sample, one side coated

Note: 4PB, four-point bending; PS, plasma sprayed. (a) particle size −50 + 40 μm. (b) particle size −63 + 50 μm

coating was deposited on the substrates on both sides for fatigue tests and on one side for four-point bending tests. There was only a negligible amount of overspray on the edges of the specimen, which was not removed.

2.1 Fatigue Testing

The fatigue samples were loaded in reversible bend (as a cantilever beam) at room temperature in a special computer-controlled electromagnetic testing device (Fig. 2, Ref 3), which was developed at the Department of Materials of the Czech Technical University. An alternating electromagnetic field induced by a pair of coils was used to deflect the free end of the specimen, which was equipped by a yoke. A resonance effect was used to achieve the required deflection amplitude, so the loading frequency was close to the actual resonance frequency of the specimen-plus-yoke system. A feedback regulation altered the loading frequency so that the deflection amplitude of the free end of the specimen remained constant. The changes in the resonance frequency of the specimen-plus-yoke system and, hence, the changes in the loading frequency depend on the fatigue crack area. Therefore, it is possible to estimate specimen damage from the change in the loading frequency.

For specimens having a thickness of 4 mm, the frequency drop of 5 Hz corresponded to relative cross-sectional damage of about 30%. Sample damage on this level is optimal for fractographic analysis. In the following text, the term "fatigue life" refers to the number of cycles preceding the 5 Hz drop in the loading frequency. More information about the fatigue testing method can be found in Ref 3.

2.2 Microhardness Profile Measurement

To estimate qualitatively the residual stress in the substrate near the substrate/coating interface, a series of microhardness measurements were performed. Compressive residual stresses should increase the microhardness of the material, whereas tensile residual stresses should result in a decrease in microhardness. To this end, a Vickers microhardness tester (O.P.L., Sopelem, Levallois-Perret, France) was used. The specimens to be measured for microhardness were cut from the upper heads of fatigued specimens, that is, from a part of the specimen that was not subject to extensive mechanical loading. The microhardness was measured on specimens that were cut transversally and on those cut on an inclined plane (a tilt of 15° to the coating surface). Approximately 30 measurements were made on each specimen. The loading force was 0.2 N for the specimen cut transversally and 5 N for the specimen cut on an inclined plane.

2.3 X-Ray Residual Stresses Measurement

The residual stresses were measured by x-ray diffraction near the surface of the coating and on the inclined plane cut of the substrate using the $\sin^2 \Psi$ method. The stress measurements were performed on the upper and lower heads of the specimen, that is, on parts of the specimen with the highest and lowest mechanical load. An x-ray diffractometer (model D500, Siemens AG, Karlsruhe, Germany) with a copper anode was used.

2.4 In Situ Bending Test

The mechanism of crack propagation under increasing static bending load was observed by in situ experiment with an SEM. A thin strip of coating-substrate composite was loaded by three-point bending in a special jig (Fig. 3) that was situated in the vacuum chamber of an SEM (JSM-50, JEOL Ltd., Tokyo, Japan), which was equipped by a custom digital image-acquisition system. Both the special loading jig and custom image acquisition system were developed in the Department of Materials of the Czech Technical University.

2.5 Fractographic and Metallographic Analysis

The crack surfaces were observed on one typical sample from each set with a SEM (JSM-840, JEOL Ltd.) in secondary electron mode. Samples with alumina coating were gold coated to prevent electrostatic charging.

One sample from each set was metallographically observed. The samples were prepared from the upper heads of the fatigue specimens to avoid the effects of loading. The cross section of the specimen was polished up to 1 μm with diamond paste and was etched in 5% nital for 20 s. The observation with the optical microscope was focused mainly on the substrate structure near the substrate/coating interface.

2.6 Four-Point Bending Tests

Young's modulus was measured using a four-point bending apparatus, used with Instron model 1362, an electromechanical testing machine (Instron Ltd., High Wycombe, U.K.). A special device (Fig. 4) was designed to achieve high accuracy for the testing of coating-substrate plate specimens. The outer span of the supports, which was 94 mm long, was divided by inner sup-

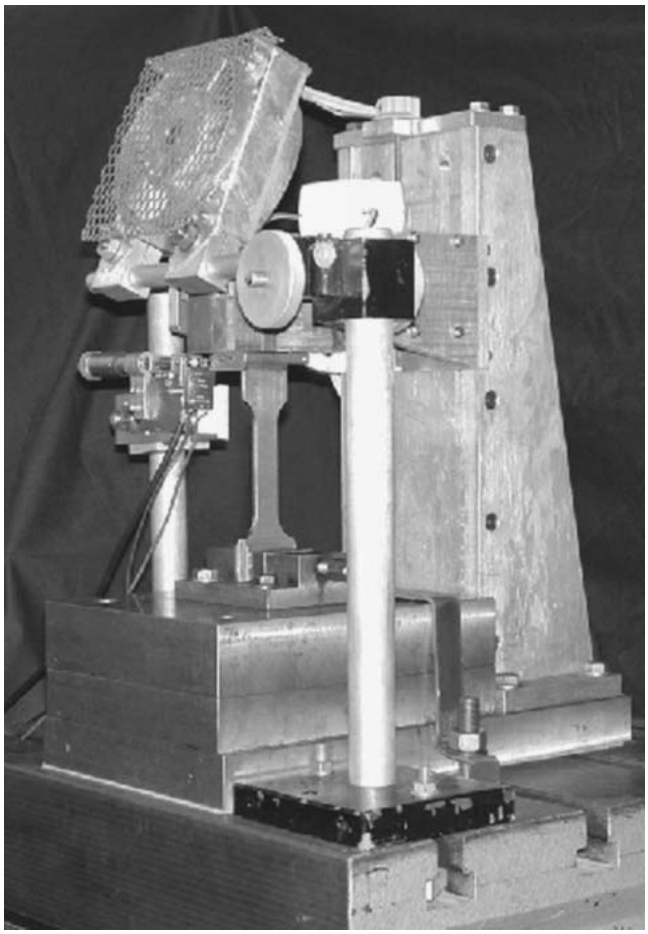

Fig. 2 The specially designed electromagnetic device "SF-test" that was used to test fatigue resistance

ports into four equidistant fractions that were each 23.5 mm in length. To eliminate the inner stiffness of the four-point bending apparatus that was used, specimen deflection was independently measured by an external strain gage. Experimental data (displacement, strain, and load) were recorded and evaluated by a special code, solving automatically systems of complicated quadratic equations that were based on a linear elastic model. Stresses in the coating were calculated using the strain values measured by a deflection gage and the previously calculated Young's modulus of the coating at a given load. The four-point bending machine was operated mainly in the position-control mode. The usual rate of displacement was 0.0063 mm/s, and the maximum loads varied between 300 and 800 N.

3. Results

3.1 Fatigue Results

The fatigue lives of specimens from the series referred to in Table 1, P, TA, 1A, 2A, and 3A, were plotted in a Weibull probability paper (Fig. 5), which clearly indicated extended fatigue lives for samples with an alumina coating. The mean values of a factor by which the fatigue life of plain specimens from each series was multiplied are presented in Fig. 6.

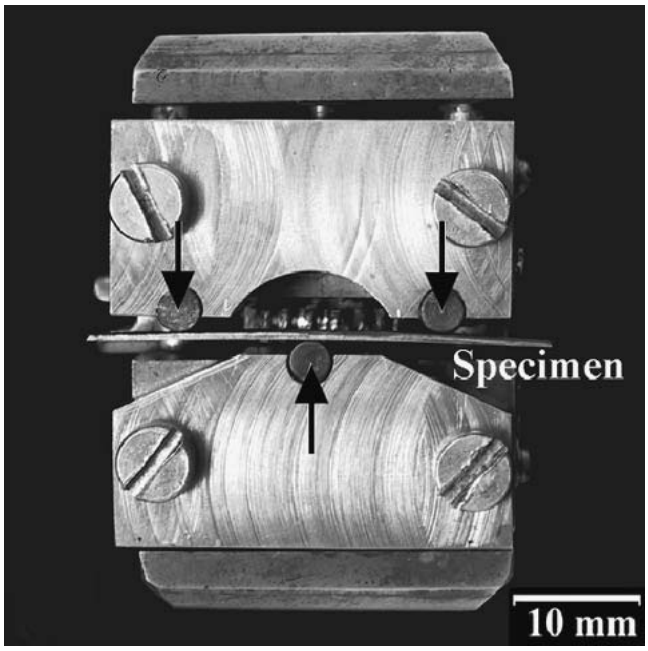

Fig. 3 Three-point bending apparatus for in situ tests (adopted from Ref 4). Arrows indicate loading forces.

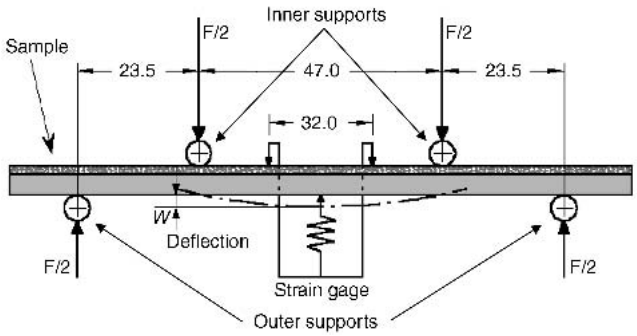

Fig. 4 Four-point bending apparatus for Young's modulus measurements (all dimensions in millimeters)

3.2 Microhardness Profile Measurement

The microhardness profile measurement clearly indicates increased microhardness values in the substrate to a depth of about 100 mm in both the 1A and TA sample sets (Fig. 7). The 1A sample set exhibits slightly higher microhardness near the substrate/coating interface than the TA sample set.

3.3 X-Ray Residual Stresses Measurement

The x-ray residual stress measurement indicated tensile residual stress at the surface of the coating for the 1A and 3A sample sets (the 2A sample set was not measured). Tensile stresses with a magnitude of about 250 MPa were present regardless of the mechanical load to which the measured area was subjected (Table 2).

The residual stress profiles measured on the inclined cross section of the substrate are presented in Fig. 8. Metallographic preparation might have influenced the residual stress; however, the residual stress gradient should remain unchanged. The com-

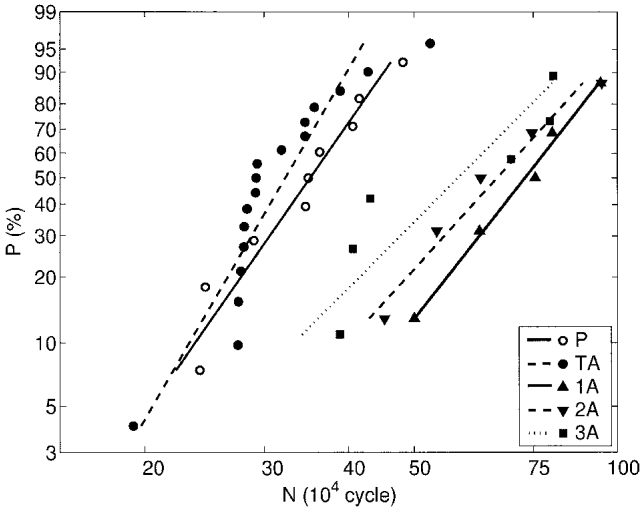

Fig. 5 The Weibull probability plot of cumulative percent failure versus the number of cycles

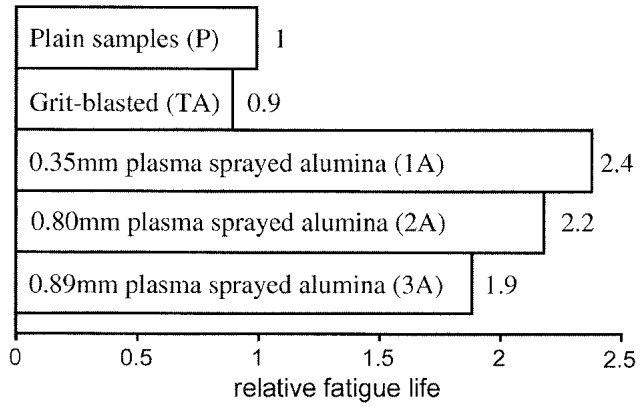

Fig. 6 The relative fatigue life of sample sets sprayed with different spraying conditions. The average fatigue life of each set is related to the average fatigue life of the plain specimen set.

pressive residual stress decreased with increasing distance from the interface. The maximum compressive residual stress reached about –250 and –300 MPa, respectively, for specimens from the TA and 1A sample sets. Reference specimens exhibited relatively constant stress field along the measured area of stress value about –150 MPa.

3.4 In Situ Bending Tests

The results of in situ observation (Fig. 9, 10b) show that the crack propagation in investigated coatings can be explained by the following mechanisms:

- *Growth and coalescence of intersplat pores and voids* (generally parallel to the substrate surface). Crack growth along the interface between the coating and the substrate also was observed if the sample deformation was high.
- *Splat breaking* (often perpendicular to substrate surface) was a very often observed phenomenon, which accomplished intersplat cracking.

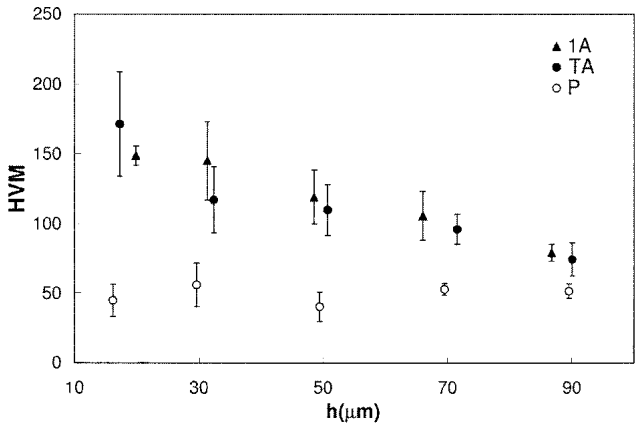

Fig. 7 Microhardness under 0.2 N load profile in the depth of substrate. Note the microhardness increase near the interface ($h = 0$).

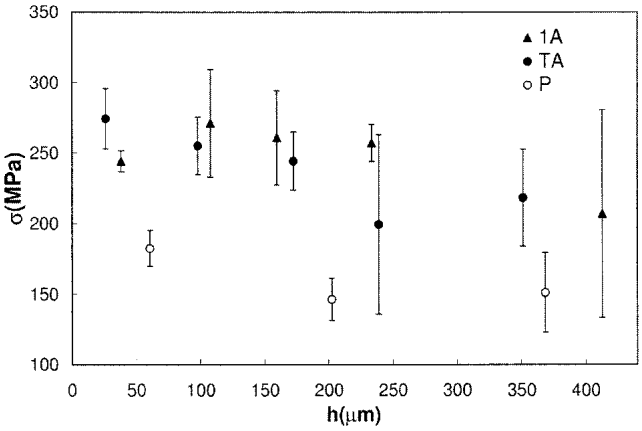

Fig. 8 The profile of residual stresses, measured by x-ray diffraction on an inclined cross section of the sample

Table 2 Residual stresses at the surface of Al_2O_3 coating

		Residual stress (σ_φ), MPa	
Set	**Part**	**Longitudinal**	**Transversal**
1A	Not loaded	+260 ± 40	+240 ± 40
	Loaded	+230 ± 30	+320 ± 40
3A	Not loaded	+210 ± 40	+260 ± 30
	Loaded	+300 ± 30	+290 ± 40

- If the loading level was high enough, crack growth into the substrate was observed.

3.5 Fractographic and Metallographic Analysis

Fatigue cracks were initiated near the edges of the specimen (Fig. 10a) and along the coating/substrate interface. Generally, the fatigue crack initiation sites in the substrate were found in the areas influenced by the processes of grit blasting and plasma spraying (grain deformation and residual stress). The fractography of the coating confirmed that the crack growth was performed by splat breaking (Fig. 10b), and by the growth and coalescence of intersplat pores and voids.

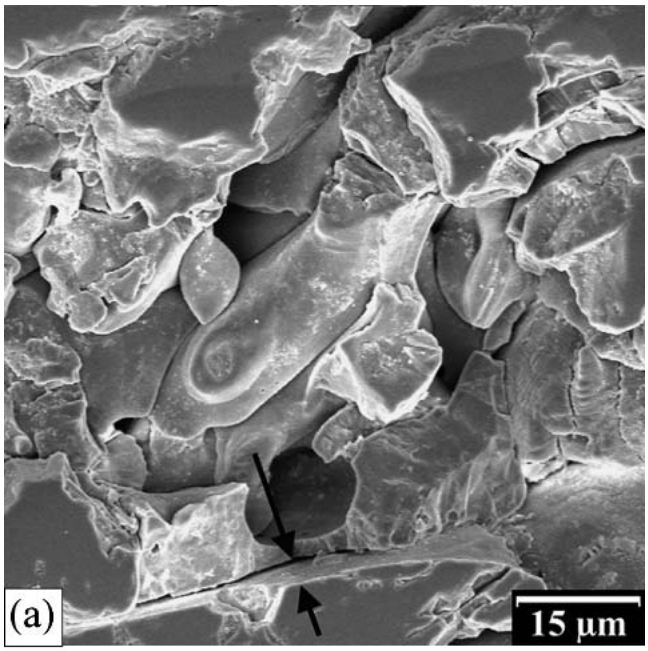

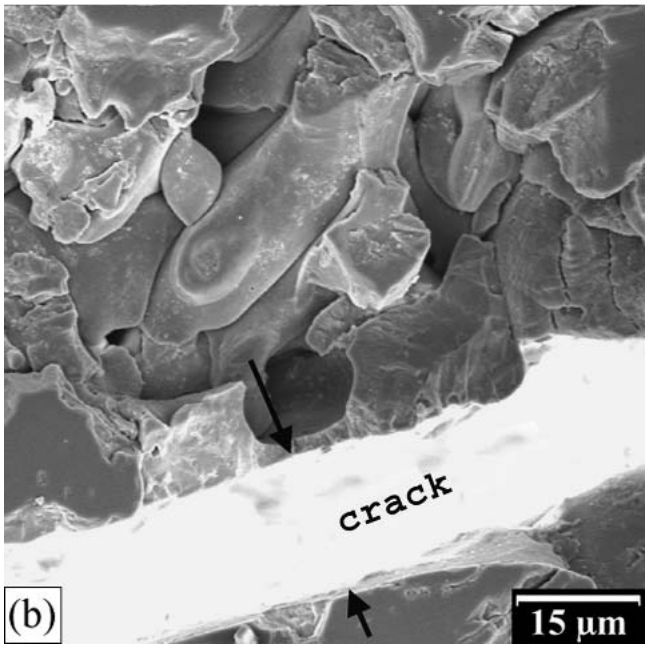

Fig. 9 Two stages (a, b) of cracking in the alumina coating on 3A sample set

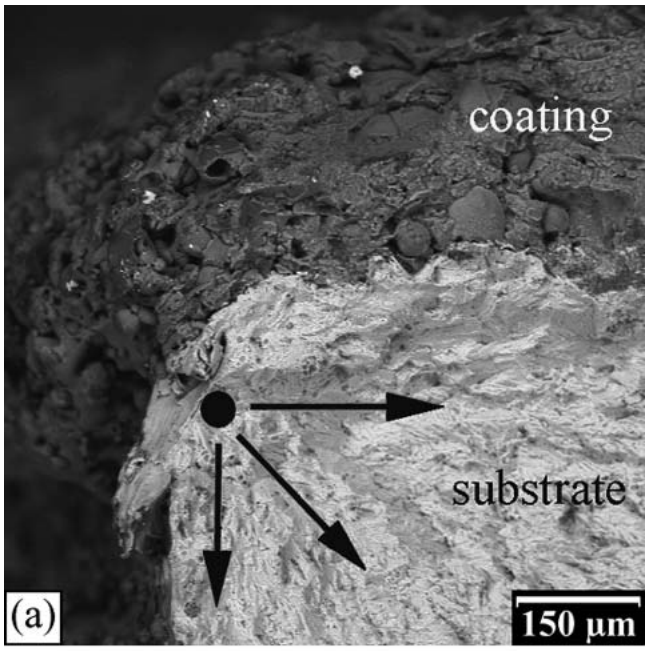

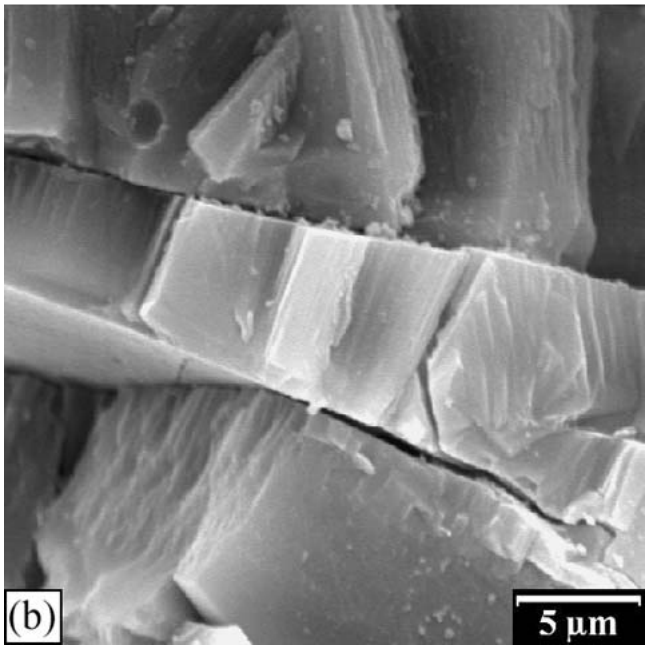

Fig. 10 SEM observation of the alumina coating obtained using the 1A sample set of parameters, indicating crack indication (a) and crack propagation through a lamella (b). The arrows show the directions of crack propagation.

Optical micrographs of polished and etched cross sections showed grain deformation near the substrate/coating interface (Fig. 11) for all specimens, with the exception of those from the reference sets P and TA. The deformation originated from grit blasting and was noticeable to a depth of about 100 mm. The substrate roughness increased dramatically after grit blasting, and Al_2O_3 particles indented during grid blasting were found on the substrate surface.

Cracking in the substrate without any noticeable coating damage also was revealed by optical micrographs.

3.6 Young's Modulus Determination

Measurements of Young's modulus of the coating were made for small and big deformations. First, Young's modulus of the coating at small deformations (less than ~0.1%) was measured. Second, the evolution of the Young's modulus of alumina coatings during high-load experiments (deformations up to 0.4%) was investigated. High-load measurements of Young's modulus were initiated by the results of the authors' preliminary experiments and also by increasing evidence in the literature (Ref 5)

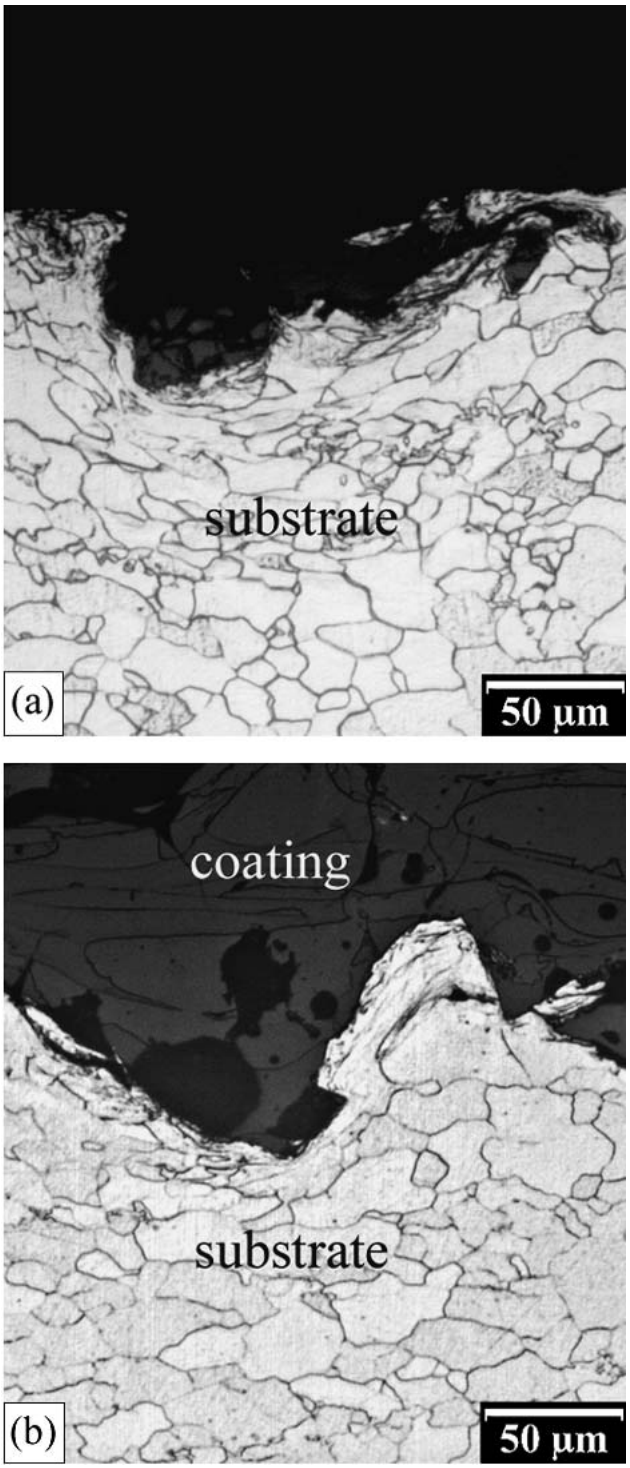

Fig. 11 Optical micrograph of a cross section of substrate/coating interface showing extensive grain deformation for both the samples sprayed using TA (a) and 1A (b) conditions

showing that the Young's modulus of thermally deposited coatings may vary at higher strains. For small deformations, results were evaluated according to a linear elastic theory, assuming a constant Young's modulus through the thickness of the coating. The Young's modulus of the alumina coating on the 1A40

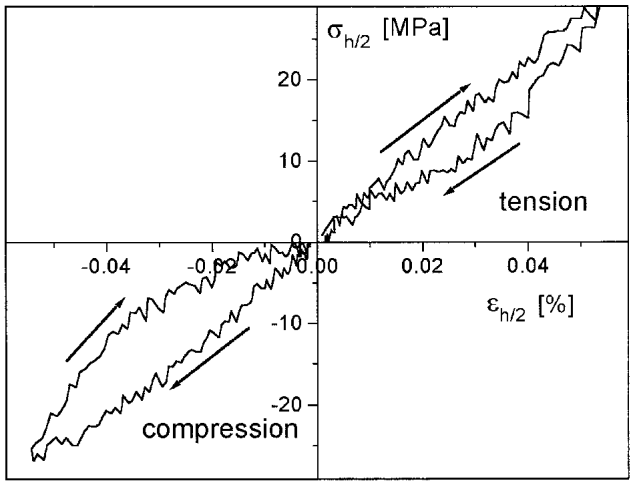

Fig. 12 The typical four-point-bending, loading-unloading curve for the 1A40 sample set

sample set was found to be $E = 45 \pm 8$ GPa. There was no remarkable difference between the Young's modulus measured during tensile or compressive loading. A typical loading-unloading curve for coating from the 1A40 sample set is shown in Fig. 12.

One can notice a relatively high scattering of data, which can be caused by a high substrate-to-coating thickness ratio (0.4-4 mm). The scattering of experimental data is further magnified by the fact that the Young's modulus of the coating is more than four times smaller than that of the steel substrate. Thus, it is obvious that the determination of the Young's modulus of thin coatings deposited on thick substrates could have led to considerable inaccuracies due to the fact that the coating represents only approximately 10% of the total stiffness of the coating-substrate system.

That is why a more appropriate substrate-to-coating thickness ratio was chosen. The Al_2O_3 coating that was deposited under the same spraying parameters and roughly the same 0.35 mm thickness on 2.5 mm thick samples (for the 1A25 sample set) exhibited a modulus of elasticity between 46 and 57 GPa. An example of the loading-unloading curve is shown in Fig. 13. A remarkable increase in the modulus of elasticity when the coating was placed in compression (57 ± 4 GPa versus 46 ± 3 GPa in tension) can be observed. Also a more favorable substrate-to-coating thickness ratio was reflected in a loading-unloading curve that was smoother than that for the 1A40 sample set (compare Fig. 12 and 13).

4. Discussion

4.1 Fatigue

Other authors have reported shorter fatigue lives for coated specimens than for uncoated specimens (Ref 6, 7). However, in the case of the investigated alumina coating, fatigue testing proved that the coated specimens exhibit considerably longer lives under fatigue conditions than those without coatings. Extended fatigue lives of coated specimens for various types of coatings also were observed in the authors' previous experiments (Ref 4).

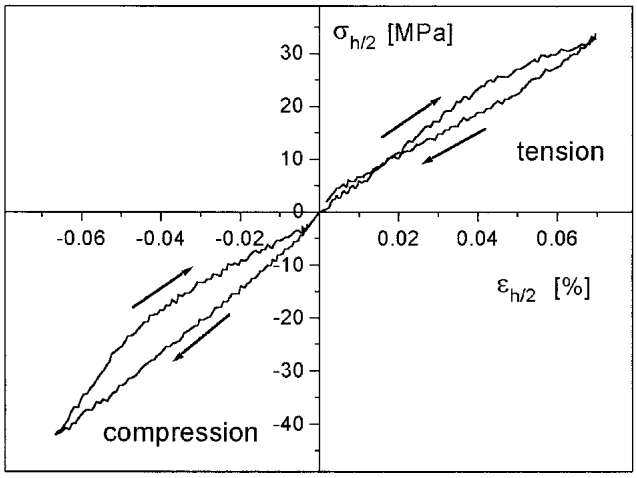

Fig. 13 Typical four-point-bending, loading-unloading curve for the 1A25 sample set

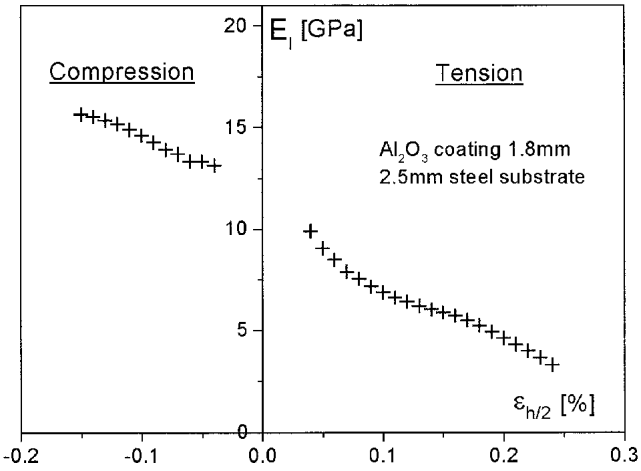

Fig. 14 The plot of the Young's modulus versus deformation in the center plane of the coating (defined as the plane perpendicular to the spray direction located in the center of the thickness (h/2) of the coating). The values for the Young's modulus at low deformations (<0.04%) are omitted for technical reasons.

The effect of grit blasting on the fatigue life of the investigated specimens is insignificant. Grit blasting invokes two major effects: compressive residual stress (indicated by the x-ray residual stress measurement and microhardness profile measurement, Fig. 7, 8) and increased surface roughness (observed on metallography specimens, Fig. 11) accompanied by stress concentrators on the rough substrate surface. Clearly, such stress concentrators will assist crack initiation. In the experiments, the two effects of grit blasting were equilibrated; therefore, the fatigue lives of grit-blasted specimens were very similar to those of the reference specimens.

The results of fractographic analysis have indicated that the fatigue lives of the investigated plasma-sprayed specimens depend mainly on the crack-initiation phase. Therefore, the extended fatigue life can be attributed to a decrease of tensile stress in the substrate near the substrate/coating interface. This decrease can be caused by residual stress originating from coating deposition or by reaction of the coating on substrate crack opening.

Compressive stress in the substrate can be a response to tensile stress in the coating that originated in the coating deposition. This could be indicated by a relatively small increase in microhardness among the grit-blasted specimens and the grit-blasted and coated specimens (Fig. 7). The results of Ref 8 show that the residual stresses in the plasma-sprayed alumina coating are relatively uniform. Therefore, the residual stress on the surface of the coating of a magnitude of about 250 MPa, which was determined by x-ray measurements, could possibly indicate the presence of increased tensile stress in the coating near the coating/substrate interface.

The nucleation of a small crack in the substrate under an undamaged coating would result in the local deformation of the substrate. Clearly, this deformation would not be possible without a reaction in the coating that would force the crack to close.

4.2 Young's Modulus

Up to 0.1% deformation of the Young's modulus was considered to be independent of loading. In the case of the Al_2O_3 coatings investigated, the Young's modulus calculated (46 GPa) was approximately six times lower than that of the bulk Al_2O_3 (300 GPa). This value confirmed the authors' previous measurements and also was reported by other researchers (Ref 1, 9). However, the inappropriate coating-to-substrate thickness ratio associated with a substantial difference between the coating and substrate Young's modulus could have led to inaccurate results. Similar results were obtained by Kucuk et al. (Ref 10) when testing a zirconia coating by four-point bending. The authors suggested that it is necessary to use the coating on a thinner substrate for a more accurate determination of the Young's modulus. Despite the fact that the values of the Young's modulus of the thick coating on the 1A40 sample set should thus be considered only as preliminary, they correspond to those of the 1A25 sample set. In contrast to the 1A40 sample set, a substantial difference between the Young's modulus values measured in tension and in compression was observed in the case of 1A25 sample set. A Young's modulus of 57 GPa was measured in compression, in contrast to 46 GPa measured in tension. This change in the value of the Young's modulus is believed to be due to the presence of intrasplat and intersplat cracks in the splat structure of the coatings (Ref 2).

The results of the authors' experiments indicate that the Young's modulus of plasma-sprayed coatings depends on the load. The threshold deformation at which the changes in Young's modulus become noticeable is about 0.1%. This behavior was well observed in samples that were identical to the 1A25 sample set, but having thick (1.8 mm) Al_2O_3 coatings. These samples were loaded up to 800 N (maximum deformation of ~0.25% in the center plane of the coating). A plot of the Young's modulus versus deformation in the center plane of the coating for such a sample is shown in Fig. 14.

Under tension conditions, the defects in the intersplat bonds (intersplat thin voids) in the coating are opened by the shear forces. The enlargement of the intersplat thin voids has a negative effect on the integrity of the coating, thus causing a drop in the Young's modulus. Such effects are strongly nonelastic in the

case of freestanding bodies; however, in the case of coatings that are bonded to the substrate, the deformation of the coating is constrained by the substrate. Therefore, the linear response of the whole substrate-coating system remains relatively unchanged. However, the changes in the coating stiffness can be measured. A partial opening of the intersplat thin voids (tensile stress) leads to a decrease in the stiffness, and partial closing (compressive stress) may lead to an increase in stiffness. It is obvious that at a certain value the changes in the coating structure start to have a permanent effect on the stiffness of the coating. From this point on, further loading would cause irreversible damage to the coating, resulting in a decrease of the Young's modulus, in some cases to zero value. The description of the Young's modulus relation to deformation at high loads will be the subject of continuing study, which will be based on the results presented in this study.

5. Conclusions

The objective of determining the effect of a plasma-sprayed alumina coating on fatigue life was accomplished for the constant-deflection bend testing of several sets of specimens, corresponding to various stages of coating application. The increase of the life of an alumina-coated specimen under fatigue conditions is clearly demonstrated by the results of the tests that were performed. Two major conclusions can be drawn from the experiments:

- The grit blasting does not significantly influence the fatigue performance of the investigated specimens.
- The application of plasma-sprayed coating increases the life of the specimen tested under fatigue conditions by about two times.

The investigation of failed specimens revealed compressive residual stress on the substrate side of the coating/substrate interface, tensile residual stress on the surface of the coating, substrate grain deformation and the mechanism of crack propagation in the coating by splat-breaking, and the coalescence of intersplat pores and voids.

The Young's modulus of the coating at small deformations ($\lesssim$0.1%) varied between 27 and 53 GPa, with an average value of 43 GPa. The analysis of the results showed that a more accurate determination of the Young's modulus requires the use of coatings on a thinner substrate. Experiments at high deformations ($\gtrsim$0.1%) confirmed the dependence of the Young's modulus on applied stress. Loading in tension caused a decrease in the Young's modulus of the coating, while loading in compression led to an increase in the Young's modulus of the coating. This behavior can be explained by the partial closing and opening of intersplat thin voids.

Acknowledgment

This research was supported by the Grant Agency of the Czech Republic (grant No. 106/01/0094, "Failure Processes in Thermally Sprayed Materials").

References

1. F. Kroupa and J. Dubský, Pressure Dependence of Young's Modulus of Thermal Sprayed Materials, *Scr. Mater.,* Vol 40 (No. 11), 1999, p 1249-1254
2. F. Kroupa and J. Plesek, Nonlinear Elastic Behavior in Compression of Thermally Sprayed Materials, *Mater. Sci. Eng., A,* Vol 328 (No. 1-2), 2002, p 1-7
3. J. Siegl, P. Kantor, and J. Adamek, Fatigue Processes in Bodies with Surface Coatings, *Proceedings of the 14th International Conference on Surface Modification Technologies,* T.S. Sudarshan and M. Jeandin, Ed., ASM International and IOM Communication Ltd., 2001, p 64-70
4. J. Siegl, P. Kantor, and J. Adamek, Investigation of Fatigue Processes in Bodies with Surface Coatings, *Acta Technica,* Vol 46, 2001, p 251-264
5. V. Harok and K. Neufuss, Elastic and Inelastic Effects in Compression in Plasma-Sprayed Ceramic Coatings, *J. Thermal Spray Technol.,* Vol 10 (No. 1), 2001, p 126-132
6. R.T.R. McGrann, D.J. Greving, J.R. Shadley, E.F. Rybicky, T.L. Kruecke, and B.E. Bodger, The Effect of Coating Residual Stress on the Fatigue Life of Thermal Spray Coated Steel and Aluminum, *Surf. Coat. Technol.,* Vol 108-109, 1998, p 59-64
7. L. Hernández, F. Oliveira, J.A. Berríros, C. Villalobos, A. Pertuz, and E.S. Puchi Cabrera, Fatigue Properties of a 4340 Steel Coated with Colmonoy 88 Deposit Applied by High-Velocity Oxygen Fuel, *Surf. Coat. Technol.,* Vol 133-134, 2000, p 68-77
8. O. Kesler, J. Matejicek, S. Sampath, S. Suresh, T. Gnaeupel-Herold, P.C. Brand, and H.J. Prask, Measurement of Residual Stress in Plasma-Sprayed Metallic, Ceramic and Composite Coatings, *Mater. Sci. Eng., A,* Vol 257 (No. 2), 1998, p 215-224
9. L. Pawlowski, *The Science and Engineering of Thermal Sprayed Coatings,* J. Wiley, 1995
10. A. Kucuk, C.C. Berndt, U. Senturk, R.S. Lima, and C.R.C. Lima, Influence of Plasma Spray Parameters on Mechanical Properties of Yttria Stabilized Zirconia Coatings: I. Four Point Bend Test, *Mater. Sci. Eng., A,* Vol 284 (No. 1-2), 2000, p 29-40